



## RAPID COMMUNICATION

# Immunogenomic classification of lung squamous cell carcinoma characterizes tumor immune microenvironment and predicts cancer therapy



Lung squamous cell carcinoma (LSCC) is the second most common histological type of non-small cell lung cancer (NSCLC) after lung adenocarcinoma, accounting for 30% of all NSCLC cases. Cytotoxic chemotherapy and radiotherapy are commonly used as adjuvant therapy following surgery for LSCC. Advanced and metastatic LSCC patients typically receive systematic therapy that consists of a platinum-based doublet. Rare mutations of two main oncogenic drivers (*EGFR* and *KRAS*) in LSCC hindered the development of molecular targeted therapies.<sup>1</sup> Cancer immunotherapy based on anti-PD-1 (programmed cell death 1)/PD-L1/CTLA-4 (cytotoxic T-lymphocyte-associated protein 4) therapies represents promising therapeutics for NSCLC patients, while obtained remission rate was unsatisfactory partly due to the heterogeneity of the tumor immune microenvironment (TIME). Therefore, comprehensive characterization of TIME in LSCC is vital to predict the responsiveness to immunotherapy and develop new effective therapies for LSCC.

Firstly, the proportions of 29 immune signatures previously described<sup>2</sup> were quantified in LSCC patients using single sample gene set enrichment analysis. Patients totaling 502 (Table S1-sheet A) were classified into distinct immunity-high ( $n = 383$ ) and immunity-low ( $n = 119$ ) subtypes by hierarchical clustering (Fig. 1A; Fig. S1A). To characterize the tumor microenvironment (TME) between two subtypes, the infiltrating stromal/immune cells as well as tumor cellularity were inferred by the ESTIMATE (Estimation of STromal and Immune cells in Malignant Tumor tissues using Expression data) algorithm. Increased immune/stromal scores were observed in the immunity-high subtype (Fig. 1B), and tumor purity was estimated to be

elevated as well (Fig. 1C). Low tumor stem cell index calculated using an innovative one-class logistic regression analysis was observed in the immunity-high subtype (Fig. S1B). Further quantification of infiltrating immune cell subsets using multiple deconvolution algorithms showed higher infiltrated total T cells, CD8<sup>+</sup> T cells, and NK cells (Fig. 1D, E) in the immunity-high subtype. Immunity-high subtype also had increased cytotoxic activities (Fig. 1F). These data suggested that patients within the immunity-high subtype retain enhanced anti-tumor immunity.

Increased infiltrating IFN $\gamma$ -expressing CD8<sup>+</sup> T cells in the TME were considered as an eventful indicator of responsiveness to immune checkpoint inhibitors (ICIs)-based therapies in NSCLC patients, and also can lead to up-regulation of *PD-1/PD-L1*.<sup>3</sup> We found that the expression of T helper 1/IFN $\gamma$  gene signatures including *IFNG*, *IFNGR1/2*, *STAT1*, and *JAK1/2* was notably increased in the immunity-high subtype (Fig. 1G). This was corroborated in a previous study presenting that high IFN $\gamma$  release could induce apoptosis of NSCLC cells by activating *JAK-STAT1*-caspase signaling. High *CXCR3* expression on activated T cells can enhance the recruitment of effector T cells into the TME in Th1 inflammatory response through binding with its interferon-inducible ligands. We found that *CXCR3* and its ligands *CXCL9*, *CXCL10*, and *CXCL11* were up-regulated in the immunity-high subtype (Fig. S1C), which might promote CD8<sup>+</sup> T cells infiltration in TME to enhance tumor killing. The expression of the T cell cytotoxicity markers (*GZMA*, *CD8A*, *PRF1*, *TBX21*, and *GATA3*) were significantly increased in the immunity-high subtype (Fig. S1D). Additionally, the stimulatory checkpoint molecules (*CD27*, *CD28*, *CD40*, *ICOS*, and *TNFRSF9*) (Fig. S1E) and the inhibitory checkpoint molecules, such as *LAG3*, *PD-1*, *PD-L1* (*CD274*), *TIM-3* (*HAVCR2*), and *CTLA-4* were significantly increased expression in the immune-high subtype

Peer review under responsibility of Chongqing Medical University.

<https://doi.org/10.1016/j.gendis.2023.01.022>

2352-3042/© 2023 The Authors. Publishing services by Elsevier B.V. on behalf of KeAi Communications Co., Ltd. This is an open access article under the CC BY-NC-ND license (<http://creativecommons.org/licenses/by-nc-nd/4.0/>).

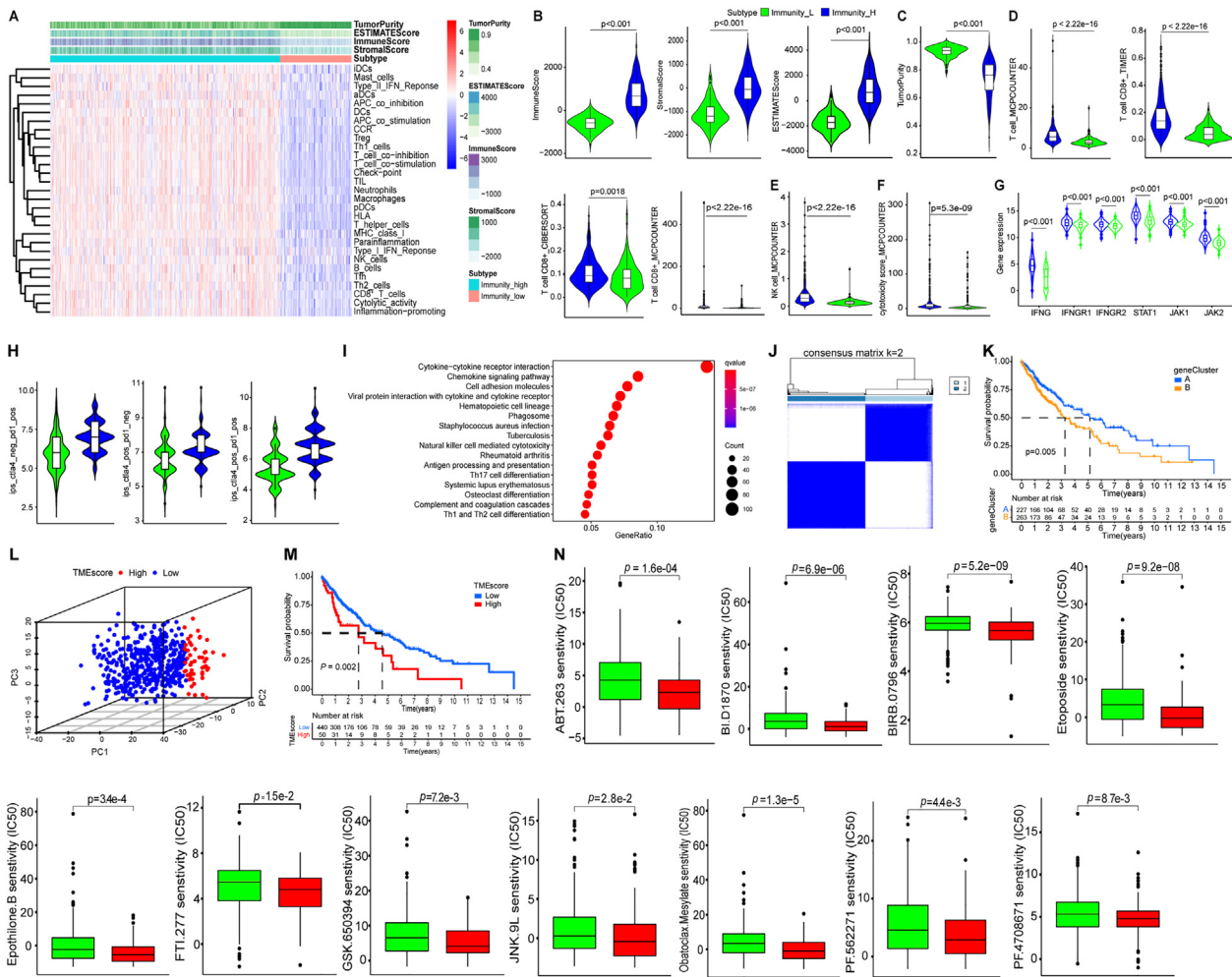


**Figure 1** Immunogenomic classification of LSCC patients characterizes tumor immune microenvironment and cancer therapy. **(A)** Hierarchical clustering of the ssGSEA scores of 29 immune signatures identified two immunity subtypes in LSCC patients. **(B)** Immune scores, stromal scores, and ESTIMATE scores of immunity-high and immunity-low subtypes. **(C)** Tumor purity of immunity-high and immunity-low subtypes. **(D)** Infiltrated total T cells and CD8<sup>+</sup> T cells calculated using TIMER, and MCPCounter and CIBERSORT deconvolution algorithms. **(E)** Infiltrated natural killer (NK) cells calculated using the MCPCounter deconvolution algorithm between immunity-high and immunity-low subtypes. **(F)** Cytotoxicity score between immunity-high and immunity-low subtypes. **(G)** The expression of the Th1/IFN $\gamma$  signatures in immunity-high and immunity-low subtypes. **(H)** Immunophenoscore (IPS) level of responsiveness to anti-PD-1 and/or anti-CTLA-4 based therapies for immunity-high and immunity-low subtypes. **(I)** Kyoto Encyclopedia of Genes and Genomes (KEGG)-based pathway analysis of differentially expressed genes (DEGs) between immunity-high and immunity-low subtypes. **(J)** Two clusters (gene cluster A and B) were identified by consensus clustering analysis based on the survival-related DEGs. **(K)** Kaplan–Meier curve of gene cluster A and B in LSCC patients. **(L)** Principal components are defined by TMEscore. **(M)** Kaplan–Meier curve of LSCC patients with high- and low-TMEscore. **(N)** Differential chemotherapeutic response based on  $IC_{50}$  available from the GDSC database between immunity-high and immunity-low subtypes.  $IC_{50}$ , half-maximal inhibitory concentration.

(Fig. S1F), suggesting immunity-low subtype might have reduced cytotoxicity due to the dysfunction of CD8<sup>+</sup> T cells. PD-L1 protein expression was also increased in the immunity-high subtype (Fig. S1G) and patients within the immunity-high subtype may benefit from anti-PD-1/PD-L1/CTLA-4 blockade. This was supported by the patients within the immunity-high subtype who have high immunophenoscore (IPS) levels (Fig. 1H).

Increasing evidence has demonstrated that dysregulation of N6-methyladenosine (m<sup>6</sup>A) messenger RNA

methylation regulators can impair the CD8<sup>+</sup> T cell anti-tumor effect and induce the resistance of anti-PD-1 therapy.<sup>4</sup> Immunity-low subtype showed significantly increased expression of m<sup>6</sup>A methylation-related genes, including *METTL3*, *YTHDC1*, and *ALKBH5*, while *FTO* showed decreased expression (Fig. S1H). This was supported by previous studies that *METTL3*, *ALKBH5*, and *FTO* play oncogenic roles in lung cancer by decreasing m<sup>6</sup>A levels. *MTTL3* depletion was reported to enhance tumor-infiltrating cytotoxic CD8<sup>+</sup> T cells and promote the production

of *IFN $\gamma$* , *CXCL9*, and *CXCL10* in TME in a mouse model. These data further demonstrate that the patients in the immunity-high subtype might have responsive TME. Human leukocyte antigen (*HLA*) molecules, a family of related proteins encoded by the major histocompatibility complex (*MHC*) genes, are tightly involved in the regulation of immune response, including antigen presentation and T-helper cell stimulation.<sup>5</sup> We found that the expression of all *HLA* genes was significantly increased in the immunity-high subtype (Fig. S1I).

Differential expression analysis was performed to investigate the difference in underlying biological processes and pathways between the two subtypes. A total of 2646 differentially expressed genes (DEGs) were identified, including 2309 up-regulated and 337 down-regulated genes (Fig. S2A). Gene functional enrichment analysis found that these DEGs were mainly enriched in immune response-related processes, such as activating cell surface receptor signaling pathway, lymphocyte-mediated immunity, regulation of immune effector process, and B cell-mediated immunity (Fig. S2B). KEGG (Kyoto Encyclopedia of Genes and Genomes) pathway analysis showed that these DEGs were involved in cytokine–cytokine receptor interaction, chemokine signaling pathway, cell adhesion molecules, natural killer cell-mediated cytotoxicity, antigen processing and presentation, and Th1 and Th2 cell differentiation (Fig. 1I). Protein–protein interaction analysis identified five transcription factors (TFs) (*FOXP3*, *CIITA*, *IKZF1*, *IRF4*, and *EOMES*) ranking the top nodes according to the degree score, all of which are involved in immune regulation (Fig. S2C). Among these DEGs, there were 22 TFs genes (Table S1-sheet B). Similar tumor immune-related pathways were identified to be enriched in the immunity-high subtype through gene set enrichment analysis (Fig. S2D).

To interrogate the potential of molecular classification for LSCC based on the DEG expression profile, and two distinct gene clusters were identified and named geneCluster A and B through unsupervised clustering (Fig. 1J). A total of 233 patients were classified into geneCluster A, which was associated with unfavorable outcomes (Fig. 1K). Most patients in geneCluster A were clustered in the immunity-low subtype (Fig. S2E). To further investigate the heterogeneity of TME that might be regulated by these phenotype-related DEGs, a TMEscore signature was generated for patients based on overall survival-related DEGs via principal component analysis (Fig. 1L and Table S1-sheet C). Patients were divided into TMEscore high and low groups using the median score as a cutoff. A set of patients with high TMEscore, accounting for ~10% of patients, had poor survival than those patients with low TMEscore (Fig. 1M). Higher immune scores of 29 immune signatures were observed in patients with high TMEscore (Fig. S3A). Differential expression analysis found that PD-L1 and CTLA-4 were highly expressed in TMEscore high patients (Fig. S3B), suggesting these patients might benefit from anti-PD-1/PD-L1/CTLA-4 blockade. This is convinced by significantly increased IPS levels in patients with high TMEscore (Fig. S3C). The alluvial diagram illustrated that most patients with high TMEscore were from the immunity-high subtype (Fig. S3D).

Chemotherapy has been used as a standard treatment modality for lung cancers. Chemotherapeutic agents for

LSCC were predicted based on the half-maximal inhibitory concentration (*IC*<sub>50</sub>) data from the Genomics of Drug Sensitivity in Cancer database using the pRRophetic package. We found that 45 chemical drugs were sensitive to patients within the immunity-high subtype by comparing the estimated *IC*<sub>50</sub>, and 26 drugs were sensitive to patients in the immunity-low subtype (Table S1-sheet D). Representative chemical drugs were displayed in Figure 1N. Several candidate compounds were predicted to be specific inhibitors in treating LSCC patients based on the DEG expression in the Broad Institute's Connectivity Map (CMap) (Fig. S3E).

Collectively, this study could provide novel insights for the characterization of TIME and prediction of cancer therapy for LSCC by immunogenomic classification. Some limitations still need to be cautious in interpreting our data as its retrospective nature. Further verification of these findings is imperative for potential clinical translation.

## Ethics declaration

This article does not contain either human or animal experiments. Written consent is not required for the current study.

## Author contributions

Conceptualization and design: Denggang Fu; Data acquisition: Denggang Fu, Biyu Zhang, Yinghua Zhang; Methodology: Denggang Fu, Biyu Zhang; Data analysis and interpretation: Denggang Fu, Biyu Zhang; Writing (original draft): Denggang Fu; Writing (review and editing): Denggang Fu, Biyu Zhang; Project administration: Jueping Feng, Denggang Fu, Hua Jiang.

## Data availability

The data analyzed in this study are available in the following repositories: TCGA (<https://portal.gdc.cancer.gov/>), Cancer Immunome Atlas (<https://tcia.at/>), Connectivity Map (<https://clue.io/cmap>), Genomics of Drug Sensitivity in Cancer (<https://www.cancerrxgene.org/>), and Broad Institute's Connectivity Map (<https://clue.io/>).

## Conflict of interests

The authors declare no potential conflict of interests.

## Appendix A. Supplementary data

Supplementary data to this article can be found online at <https://doi.org/10.1016/j.jgendis.2023.01.022>.

## References

1. Rekhtman N, Paik PK, Arcila ME, et al. Clarifying the spectrum of driver oncogene mutations in biomarker-verified squamous carcinoma of lung: lack of EGFR/KRAS and presence of PIK3CA/AKT1 mutations. *Clin Cancer Res.* 2012;18(4):1167–1176.

2. He Y, Jiang Z, Chen C, et al. Classification of triple-negative breast cancers based on Immunogenomic profiling. *J Exp Clin Cancer Res.* 2018;37:327.
3. Karachaliou N, Gonzalez-Cao M, Crespo G, et al. Interferon gamma, an important marker of response to immune checkpoint blockade in non-small cell lung cancer and melanoma patients. *Ther Adv Med Oncol.* 2018;10:1758834017749748.
4. Li X, Ma S, Deng Y, et al. Targeting the RNA m<sup>6</sup>A modification for cancer immunotherapy. *Mol Cancer.* 2022;21:76.
5. Sabbatino F, Liguori L, Polcaro G, et al. Role of human leukocyte antigen system as a predictive biomarker for checkpoint-based immunotherapy in cancer patients. *Int J Mol Sci.* 2020;21(19):7295.

Denggang Fu <sup>a,\*\*\*</sup>, Biyu Zhang <sup>b</sup>, Yinghua Zhang <sup>a</sup>,  
Jueping Feng <sup>c,\*</sup>, Hua Jiang <sup>a,\*\*</sup>

<sup>a</sup> *School of Medicine, Indiana University, Indianapolis, IN 46202, United States*

<sup>b</sup> *School of Chemical Engineering & Pharmacy, Wuhan Institute of Technology, Wuhan, Hubei 430205, China*  
<sup>c</sup> *Wuhan Fourth Hospital, Wuhan, Hubei 430033, China*

\*Corresponding author. Department of Oncology, Wuhan Fourth Hospital, No. 76, Jiefang Avenue, Wuhan, Hubei 430034, China.

\*\*Corresponding author. School of Medicine, Indiana University, 1044 W. Walnut Street, Indianapolis, IN 46202, USA.

\*\*\*Corresponding author.

*E-mail addresses:* [fdgszxy@163.com](mailto:fdgszxy@163.com) (D. Fu), [fengjuepinguai@163.com](mailto:fengjuepinguai@163.com) (J. Feng), [jianghub123@gmail.com](mailto:jianghub123@gmail.com) (H. Jiang)

6 June 2022

Available online 28 March 2023